ACTS Mobile Propagation Campaign

Julius Goldhirsh
Applied Physics Laboratory, The Johns Hopkins University
Johns Hopkins Road, Laurel, Maryland 20723-6099

Wolfhard J. Vogel, Geoffrey W. Torrence
Electrical Engineering Research Laboratory, The University of Texas at Austin
10100 Burnet Road, Austin, Texas, 78758-4497

Abstract

Preliminary results are presented for three propagation measurement campaigns involving a mobile receiving laboratory and 20 GHz transmissions from the Advanced Communications Technology Satellite (ACTS). Four 1994 campaigns were executed during weekly periods in and around Austin, Texas in February and May, in Central Maryland during March, and in Fairbanks, Alaska and environs in June. Measurements tested the following effects at 20 GHz: (1) attenuation due to roadside trees with and without foliage, (2) multipath effects for scenarios in which line-of-sight paths were unshadowed, (3) fades due to terrain and roadside obstacles, (4) fades due to structures in urban environs, (5) single tree attenuation, (6) effects of fading at low elevation angles (8° in Fairbanks, Alaska) and high elevation angles (55° in Austin, Texas). Results presented here cover sampled measurements in Austin, Texas for foliage and non-foliage cases and in Central Maryland for non-foliage runs.

1.0 Objectives

The objectives of the 20 GHz ACTS mobile propagation campaigns are to measure and analyze fading effects for the following scenarios: (1) roadside trees in rural regions, (2) trees near homes and structures in suburban communities, (3) trees with and without foliage, (4) line-of-sight elevation angles at low (8°) and high (55°) values, (5) highway obstacles such as signs, overpasses, and terrain, and (6) buildings and other structures in urban regions. The analysis involves examining multipath, shadowing, and blockage effects and extending to K-Band previous models valid at the lower UHF to S-Band [1-3].

During the first six months of 1994, four mobile propagation measurement campaigns were successfully executed by investigators from the Electrical Engineering Research Laboratory (EERL) of The University of Texas at Austin and the Applied Physics Laboratory of The Johns Hopkins University, enabling all of the above objectives to be realized. In this paper, we describe the mobile propagation system and present preliminary results associated with objectives (1)–(3).

2.0 Overview of Campaigns

An overview of the ACTS mobile propagation campaign locations, dates, elevation angles, and foliage condition is shown in Table 1. In total, four field tests were conducted during the first six months of 1994. Each test consisted of five contiguous days on which approximately four hours of measurements were made. Two field tests were undertaken in Austin, Texas where the elevation angle was approximately 55°; one during February when the deciduous trees were bare, and another during May when the deciduous trees were in full blossom. Measurements were made within the city of Austin as well as nearby suburban and rural environs. In March, tests were made in Central Maryland along the same system of roads where mobile propagation measurements were previously made at UHF and L-Band by the authors [1,3-5]. The rationale for replicating the same system of roads was to combine the results of previous measurements so that developed models could be extended to K-Band (20 GHz). In addition, measurements were made within the cities of Baltimore and Washington, DC, as well as suburban and rural communities in the vicinity of these cities.

Table 1: Locations, dates, elevation angles, and condition of foliage for 1994 ACTS mobile propagation campaigns.

Site Location	**Date (1994)**	**Elevation Angle (°)**	**Deciduous Trees**
Austin, Texas	February 14–18	54.5°	Bare
Central, Maryland	March 14–18	38.7°	Bare
Austin, Texas	May 2–6	54.5°	Full Bloom
Fairbanks, Alaska	June 6–10	7.9°	Full Bloom

3.0 Experimental Aspects

3.1 Configuration

In Figure 1 is depicted the general configuration associated with the ACTS mobile propagation campaign. A CW signal from a tone generator at approximately 3.4 GHz was injected at the upconverter input of the Link Evaluation Terminal at the NASA Lewis Research Center in Cleveland, Ohio. This resulted in an uplink signal of approximately 30 GHz and a downlink transmission at approximately 20 GHz employing the microwave switch matrix mode of ACTS. These downlink signals were received at either Austin Texas, Fairbanks

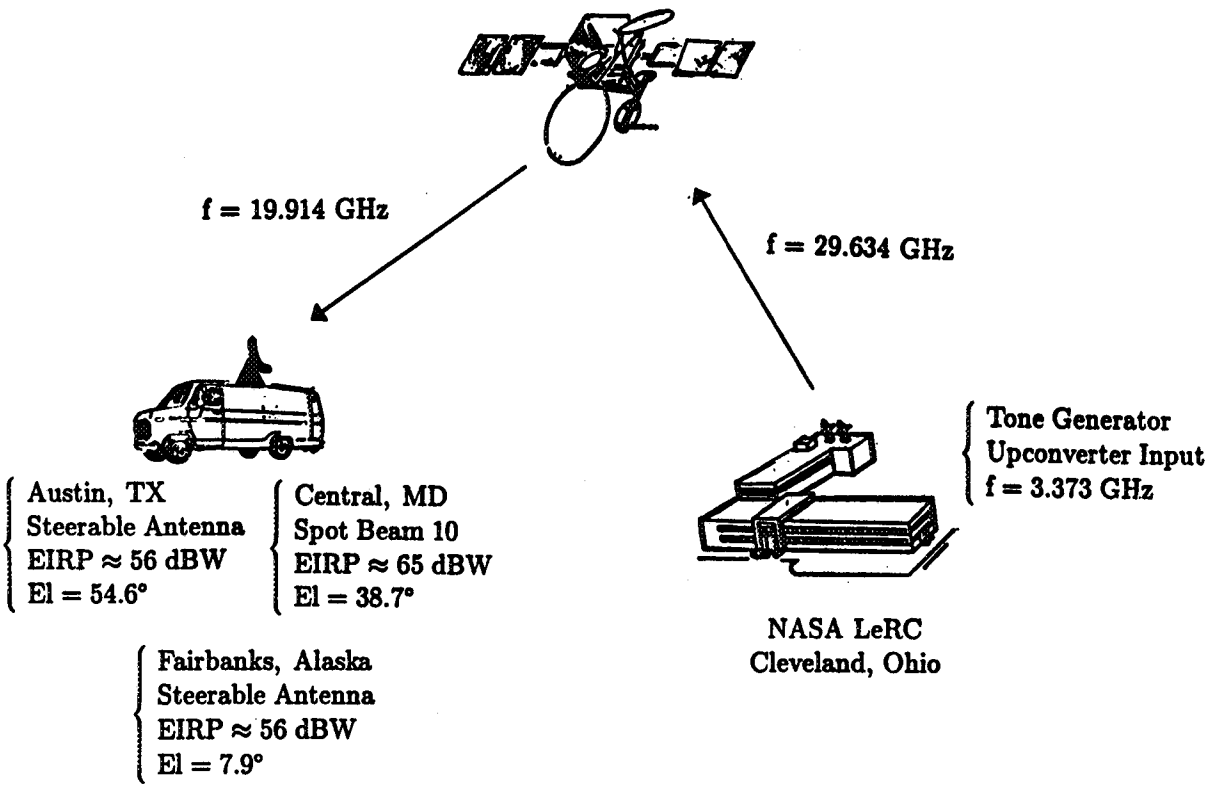

Figure 1: Experimental configuration for the ACTS Mobile Propagation Campaign.

Alaska using the steerable antenna or Central MD employing a spot beam antenna. The EIRP of the spot beam antenna (Central Maryland) was approximately 9 dB greater than that of the steerable antenna.

3.2 Link Budget

A summary of the link budget parameters is given in Table 2 for the different site locations. Utilizing a receiving horn antenna with a 1.5 inch aperture, we achieved a beamwidth of 27° and antenna gain of approximately 16 dB. With a 400 Hz bandwidth, the carrier-to-noise ratios were in excess of 30 dB in Austin Texas and Alaska and greater than 40 dB in Central Maryland. Measurements at these locations confirmed these carrier-to-noise ratios.

3.3 Elements of the Antenna Tracking System

The passive tracking system has as major elements an angular rate sensor, a flux gate compass, a horizontal rotary turn-table and a computer which points the antenna towards the satellite given the known coordinates of the satellite and the receiver location. Absolute tracking in azimuth is maintained to within a few degrees. Because the receiving antenna beamwidth is approximately 27°, the peak gain variability due to pointing errors was generally less than 1 dB for most road and city driving conditions.

The antenna and angular rate sensor rest on the rotary table which is driven by a step-motor system. When the vehicle under the rotary table turns, the rate sensor develops an output voltage proportional to the angular turn rate. This voltage is integrated to give a "turning angle" voltage which is fed into a frequency converter whose output gives a series of pulses at a frequency proportional to the turning angle. These pulses and a direction signal are interfaced with the stepping motor driver such that the rotary table is driven in the direction reducing the turning angle. When the error angle reduces to zero, no further pulses are injected into the stepping motor driver. Because the rate sensor experiences drift, the computer system also senses the drift rate relative to the average absolute vehicle direction received with a flux-gate compass mounted to the vehicle. It subsequently compensates the drift and the antenna is pointed in the correct direction. An algorithm mitigates compass errors caused by magnetic anomalies due to roadside structures.

3.4 Elements of the Receiver System/Data Acquisition System

The major elements of the receiver system are a microwave spectrum analyzer, a frequency synthesizer, the aforementioned antenna tracker system, a low noise frequency down-converter, an intermediate frequency stage with automatic frequency control (AFC), and a PC-based data acquisition system. Ancillary sensors give vehicle speed and direction. The receiver operates at 19.914 GHz, has a nominal noise bandwidth of 400 Hz, and measures both in-phase and quadrature-phase voltages at a sampling rate of 1000 Hz. The AFC tracks the satellite frequency and compensates for Doppler shift due to relative vehicle motion over a ± 1000 Hz capture range.

The resulting propagation data are stored on the computer's hard disk which has the

capacity to hold over four hours of continuous data. The time, vehicle speed, and vehicle direction are stored once per second and the antenna pointing parameters are stored at a 5 Hz rate. More complete details of the antenna tracker system and receiver system are given by Goldhirsh et al. [6].

Table 2: ACTS 1994 mobile propagation link budgets.

PARAMETER	BOTH SITES	TX Austin	MD Central	AK Fairbanks
Satellite:				
Longitude (°W)	100			
Downlink Frequency (GHz)	19.914			
Uplink Frequency (GHz)	29.634			
Polarization	Vertical			
Receiver Geometry:				
Latitude (°)N		30.4	39.25	65.0
Longitude (°)W		97.7	77.0	147.7
Elevation (°)		54.5	38.7	7.9
Azimuth (°)		184.5	213.9	129.5
Receiver Parameters:				
Polarization	Circular			
Antenna Efficiency	0.6			
Antenna Diameter (in)	1.5			
Antenna Gain (dB)	15.8			
Beamwidth (°)	27			
System Temperature K	430			
Link Budget:				
EIRP (dBW)		56	65	56
Polarization Loss (dB)	3			
Free Space Loss (dB)		−209.7	−210.0	−210.6
Atmospheric Gas Loss (dB)		0.4	0.5	2.2
Radome Loss (dB)	2.0			
Mobile G/T (dB/K)	−10.5			
Signal Power Received (dBW)		−143.3	−134.7	−146.0
Noise Power (dBW/Hz)	−202.2			
Carrier/Noise (dB per Hz)		58.9	67.5	56.2
Carrier/Noise (dB; 400 Hz)		**32.9**	**41.5**	**30.2**

4.0 Measurement Results

4.1 Fading Due to Roadside Trees with Foliage

In February 1994, the attenuation effects of an approximate 8 km stretch of a tree lined

road were measured in Bastrop, which is located approximately 30 km southeast of Austin. The road examined (Route 21) is comprised of two lanes in each direction with a median strip containing trees. Both the roadside and median strip contain approximately 75% evergreens known as loblolly pines (*Pinus taeda*). This is a coniferous tree predominant in the southeastern United States which contains bundles of stout often twisted needles and blackish-gray bark. The canopies of these trees were relatively closely spaced with overhanging regions in which they often formed a virtual tunnel of foliage above the road.

Shown in Figure 2 are fade-time series representations, where the vertical scale is the signal level relative to the unshadowed case, and the abscissa is elapsed time covering an approximate ten minute period. Three sets of curves are shown; the top and bottom curves (thin curves) represent the maximum and minimum signal levels, respectively, derived from 1000 samples during each second. The thick middle curve represents the one second average of the 1000 samples. The "average" relative signal level is shown to vary between 0 and -20 dB during the run, whereas the "minimum" relative signal level frequently is smaller than -30 dB. The "maximum" curve represents the largest signal received during the one second interval and this signal ranges from approximately $+4$ dB multipath enhancement to approximately -11 dB signal loss. The average speed of the vehicle was 32 mph for this run.

In Figure 3 are given cumulative distributions for the mobile Bastrop run (dashed curve) and two static runs obtained previously employing a fixed 20 GHz source and receiver [7]. The dot-dashed curve corresponds to an unshadowed line-of-sight distribution signifying multipath fading conditions, and the solid curve is a static distribution for a pecan tree with foliage representing attenuation due to shadowing. The ordinate for the mobile run case (Bastrop, Texas) represents the percentage of distance for which the fade is greater than the abscissa, whereas the static runs represent the percentage of shadowed locations in which the fade is greater than the abscissa.

The relative azimuth angle between the vehicle direction and the satellite ranged from 38°–80° with an average of approximately 57°, where 90° represents the case in which the line-of-sight path is orthogonal to the line of roadside trees. The slopes for the first few dB of the "clear line-of-sight" and the "pine tree" distributions are similar, indicating multipath effects for the Bastrop run. On the other hand, the slopes of the pine tree run distribution for fades in excess of 5 dB tend to match those for the pecan distribution, signifying the shadowing effects. Hence, the 20 GHz Bastrop distribution may be separated into two segments separated by an inflection region; an approximately exponential multipath part and a shadowing part, which at fades exceeding 10 dB is also exponential. We note that for 10% of the driving distance, the fades were in excess of 15 dB. Since the elevation angle was relatively high (approximately 55°), the distribution fade depth is nevertheless mitigated relative to lower angle scenarios.

The matching of distribution slopes for multipath and shadowing cases may be demonstrated using the following simple modeling concepts. We assume that the trees are identical and equally spaced with shadowing arising due to optical blockage by the tree foliage and

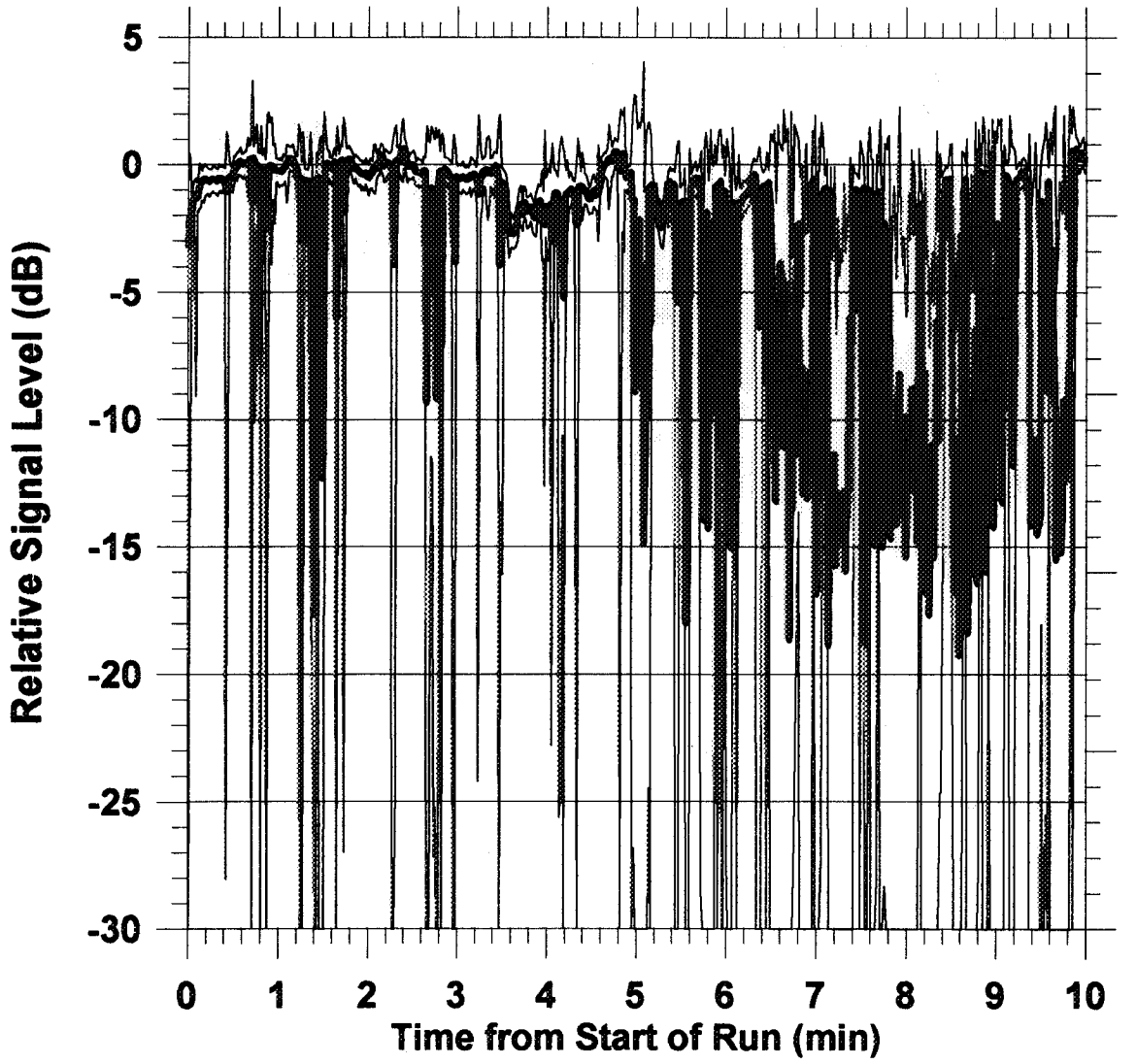

Figure 2: Relative signal time-series of maximum, minimum, and average levels for a 10 minute run (32 km) along an evergreen tree-lined road in Bastrop, Texas in February 1994.

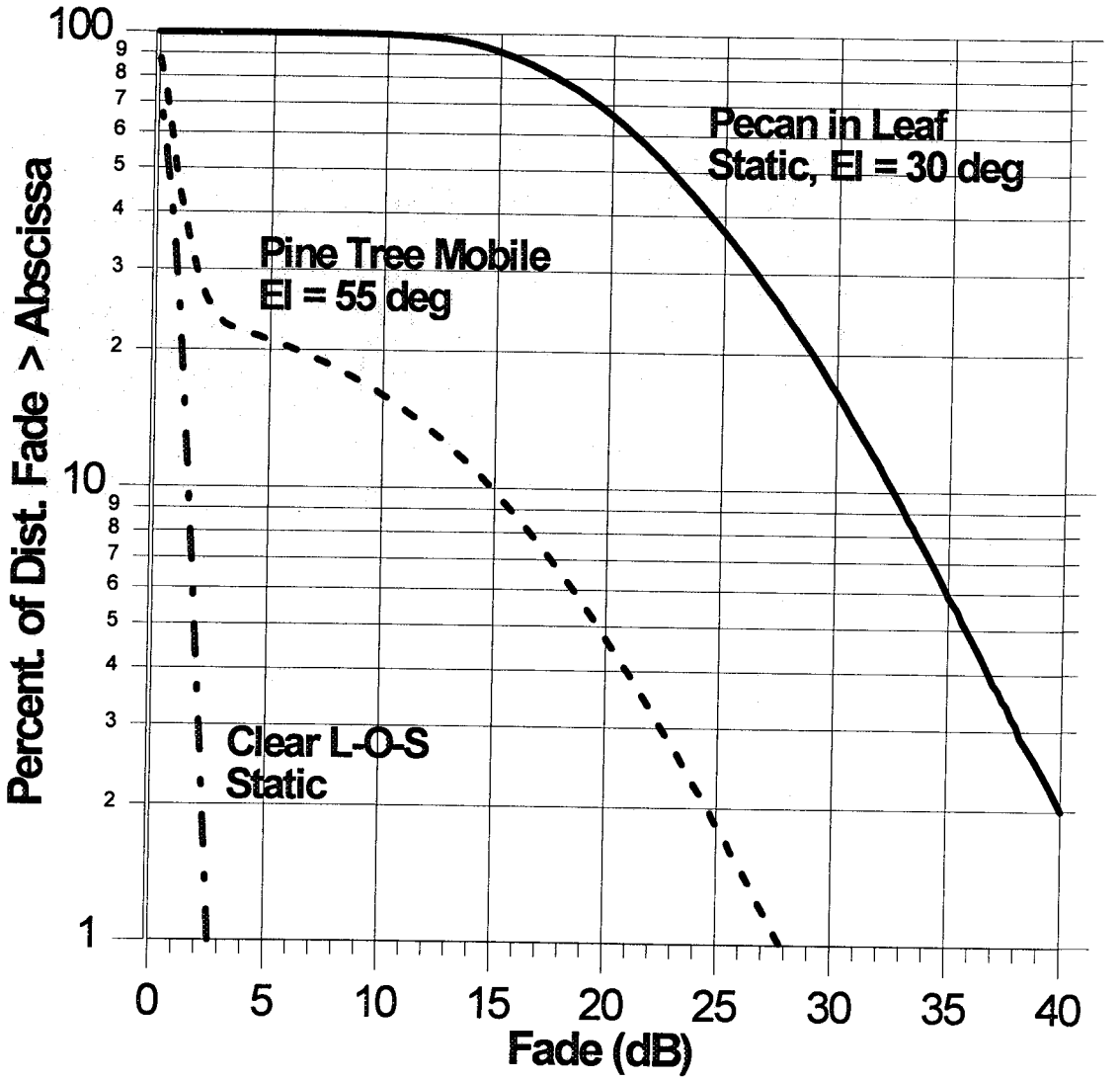

Figure 3: Cumulative distribution (dashed curve) for a 10 minute run (32 km) of an evergreen tree-lined road in Bastrop, Texas in February 1994. Also shown are static distributiond for a pecan with foliage (solid curve) and a clear line-of-sight case.

only multipath occurring during times the line-of-sight path is pointing in between the tree canopies. An expression for total shadowing probability may then be derived which is equal to the shadowing probability for a single tree times a constant factor containing the combined effects of all the trees. On a logarithmic scale, the slope of the distribution is maintained and the constant factor translates the curve up or down. An analogous methodology may be employed for the multipath case. Here, the resultant probability may be demonstrated to relate to the probability for a single multipath scenario corresponding to unshadowed line-of-sight propagation between a single pair of tree canopies times a constant representing the combined effects caused by all such scenarios in the run. The multipath distribution plotted on a logarithmic scale will have a slope for a single tree case identical to the slope of the distribution for the multiple tree scenario.

4.2 Fading Along Rural and Highway Roads

A stretch of road in Central Maryland was examined (Route 108) which is a relatively narrow, has one lane in each direction, and contains approximately 55% roadside deciduous trees. The sampled runs along Route 108 corresponded to directions southwest and northeast between Route 32 and Route 97, a distance of approximately 15 km in which the satellite path intersected the roadside trees and obstacles broadside. During the sampling period (March, 1994), the deciduous trees were without foliage.

In Figure 4 is shown an 18 minute time-series fade example for the case in which the vehicle was traveling in the northeast direction and the satellite path cut the line of roadside trees from the right. This scenario approximately replicates runs previously executed at UHF and L band employing helicopter and satellite platforms [1, 3-5]. As in Figure 2, the top and bottom thin curves represent the maximum and minimum signal levels for each 1 second period and the thick curve corresponds to the one second average. We note that occasionally average relative signal levels smaller than -25 dB occur.

In contradistinction, Figure 5 shows a set of time series corresponding to Route 295, driving south in the right lane, with the satellite generally directly in front of the vehicle and occasionally to the right. Route 295 is a four lane highway connecting Baltimore, Maryland and Washington, DC, having two lanes in each direction. The roadside foliage optical shadowing for the Route 295 run was approximately 75% as opposed to 55% along Route 108. Nevertheless, we observe significantly less fading for Route 295 because the line-of-sight paths to the satellite minimally cut the tree lines and were generally unshadowed.

In Figure 6 we combine the cumulative distributions for Route 295 (dashed) and Route 108 (solid). Shown also is the distribution for the Bastrop, Texas run (dashed-dot curve), which corresponded to a higher elevation case with trees in foliage. The following features are evident: (1) All the distributions show an inflection at approximately 3 dB separating multipath from shadowing. (2) Although Route 295 has the largest roadside tree population, fade levels are smallest because the line-of-sight path to the satellite was generally unshadowed (i.e., satellite in front of vehicle). (3) The Bastrop run showed the largest fades at percentages of 20% and smaller because this run was one in which the roadside trees contained foliage and

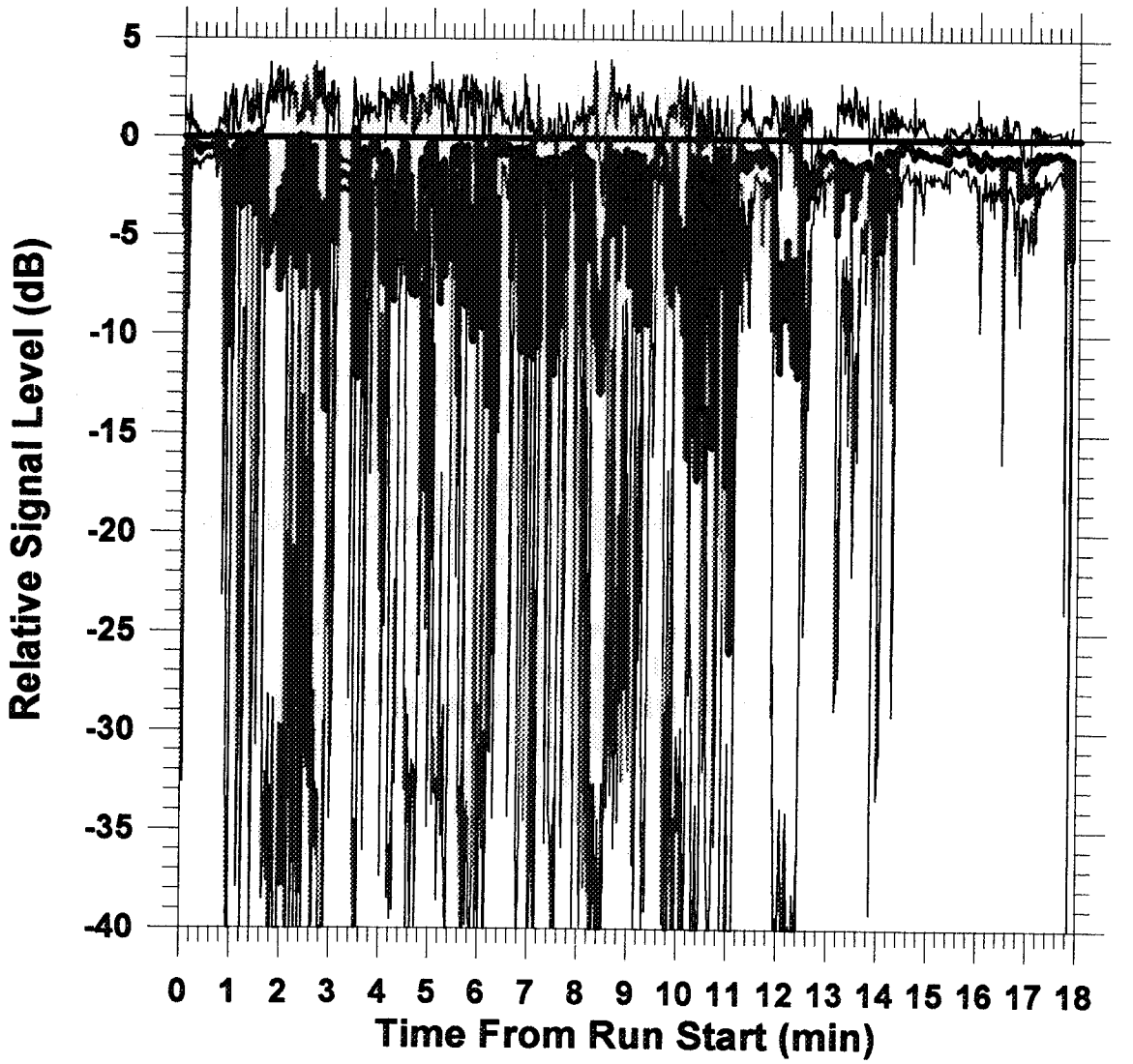

Figure 4: Relative signal time-series of maximum, minimum, and average levels for an 18 minute run (15 km) along Route 108 in Central Maryland which contains 55% deciduous trees.

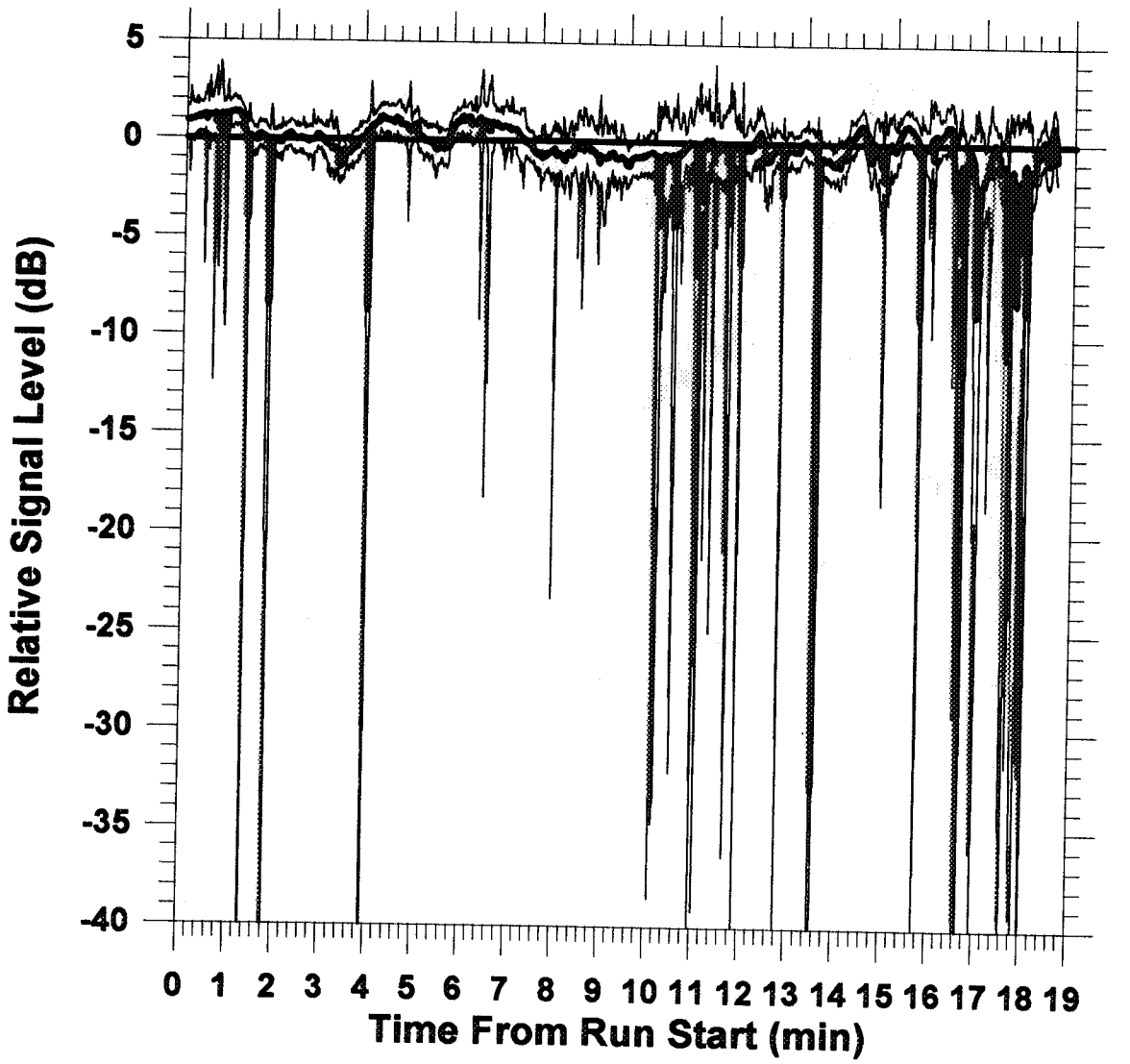

Figure 5: Relative signal time-series of maximum, minimum, and average levels for a 19 minute run (25 km) along Route 295 in Central Maryland which contains 75% deciduous trees.

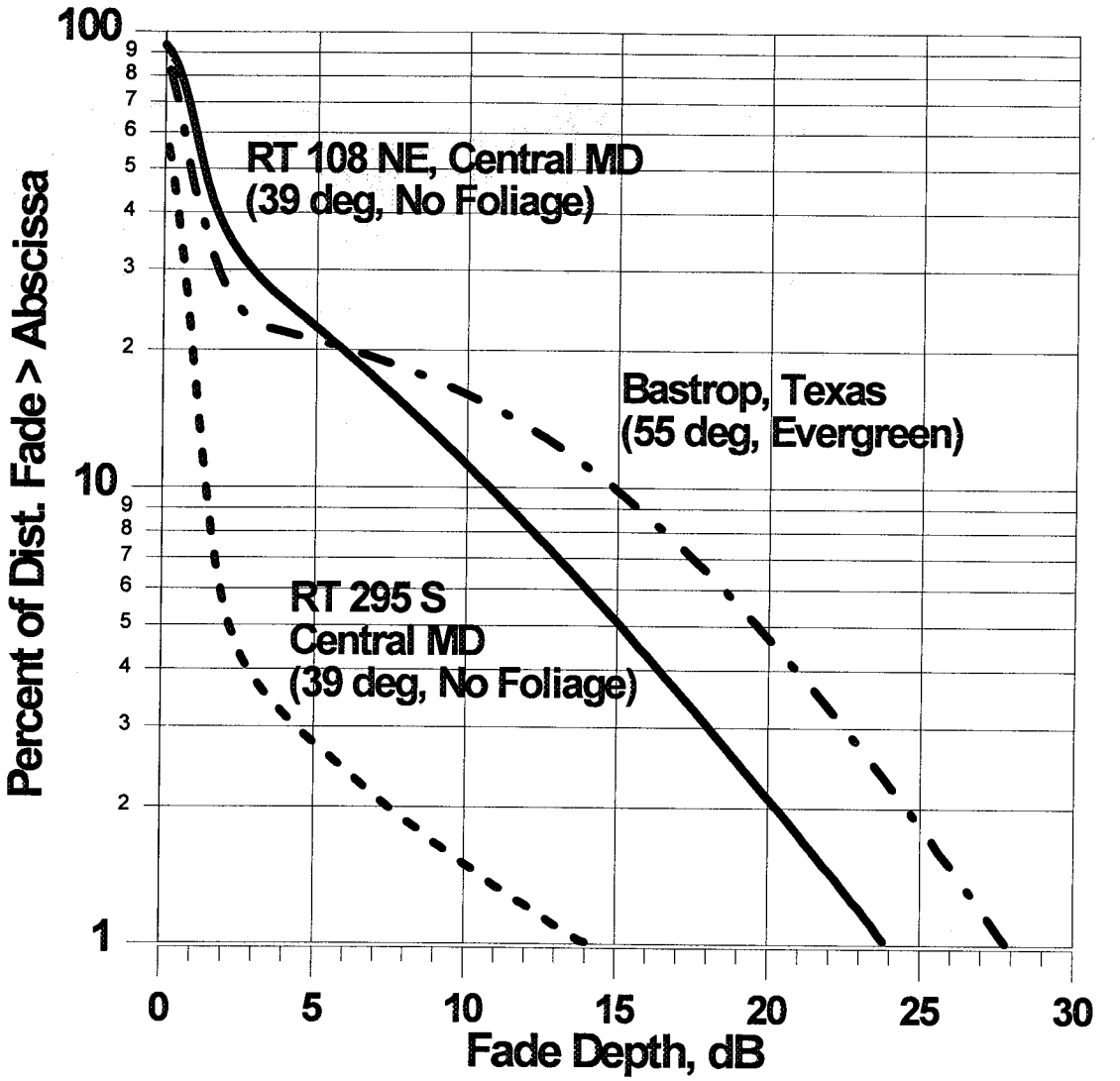

Figure 6: Comparison of cumulative fade distributions for Routes 295 and 108 in Central Maryland (no foliage) and Route 21 in Bastrop, Texas (foliage).

the line-of-sight path generally passed through the canopies. Nevertheless, the level of fades was mitigated because the higher elevation angle (55°) resulted in a reduced shadowing path length through the canopies.

4.3 Effects of Foliage on Fading

To quantify the effects of foliage during mobile runs, measurements were examined of the same tree-lined suburban streets obtained in Austin, Texas in February and May of 1994 during which time the trees were "without" and "with" foliage, respectively. As an example, we present here the foliage effects for 42nd Street between Duval and Avenue A, a stretch of road which is 0.75 km long, and is directed approximately east-west. The example run considered corresponds to the case where the receiving van was moving westward, where the line-of-sight path was above the roof-tops of the homes, but passed through the canopies of dense overhanging roadside trees (approximately 90% population) which were primarily pecan.

In Figure 7 are time series runs depicting the average 1 s relative signal levels for the foliage and non foliage cases which exhibit remarkable differences. We note the average foliage relative signal level (thick curve) is smaller than -18 dB, whereas the non-foliage relative signal level (thin curve) is greater than -9 dB. The fading effects difference between the foliage and non-foliage cases are further emphasized in Figure 8, which shows the cumulative distributions for both runs. The foliage distribution (solid curve) exhibits fades which are more than double those of the non-foliage case (dashed curve) for percentages of 50% and smaller. These results are consistent with 20 GHz signal tree measurements made previously for the static case by Vogel and Goldhirsh [7].

The effects of foliage on 20 GHz fading is very much different than those at UHF (870 MHz). Increases of fading of only approximately 25% were noted at 870 MHz [5]. The differences are explained in terms of the wavelength size relative to the spacing between branches (non-foliage case) and leaves (foliage case). At 870 MHz, the wavelength is approximately 35 cm and the spacing between branches is generally smaller than a wavelength. Hence, for both the foliage and non-foliage cases at 870 MHz, the dominant fading is due to the wood part of the tree. On the other hand at 20 GHz, the wavelength is 1.5 cm and the spacing between branches generally tends to be larger resulting in mitigated attenuation vis-a-vis the UHF non-foliage case. An analog to the above corresponds to the example of propagation through a conducting screen where minimal and maximum attenuation occur when the screen segments are large and small, respectively, relative to a wavelength. When the trees are in full foliage, the leave spacings are generally small relative to a wavelength for the 20 GHz transmissions, and hence the signal experiences substantially greater attenuation than for the non-foliage case.

5.0 Summary and Conclusions

Assuming communications between a satellite and a mobile vehicle with a 90% connectivity, fade margins at 20 GHz should be capable of compensating for 15-25 dB of tree shadowing for worst-case earth-satellite path aspects (Figures 6 and 8) when trees are in full

foliage, and 7-11 dB when trees are without leaves (Figures 8 and 6). The 20 GHz cumulative distributions show two characteristic segments separated by distinct curve inflections at approximately 3 dB (Figure 6). Fade levels smaller than 3 dB tend to be characterized by multipath fading, whereas larger fading is representative of attenuation due to shadowing. Large differences in the cumulative distributions were observed for the same tree runs during different seasons in which the trees were devoid of leaves (February) and were in full blossom (May) (Figure 8). For percentages of 50% and smaller, the fading levels with leaves were more than double those without leaves. This result is in contradistinction to the UHF case (870 MHz), where the foliage case resulted in only a 25% increase relative to the non-foliage case [5]. These differences are explained in terms of the relative wavelength size and the spacing between branches and leaves. Further efforts are planned to analyze a larger data set and address the objectives cited in Section 1.0

6.0 Acknowledgements

This effort was supported by NASA Lewis Research Center, Cleveland, Ohio under Contract N00039-91-C-0001 for the Applied Physics Laboratory, The Johns Hopkins University and Contract NAS3-26403 for the Electrical Engineering Research Laboratory, The University of Texas at Austin.

7.0 References

1 Goldhirsh, J. and W. J. Vogel, "Propagation Effects for Land Mobile Satellite Systems: Overview of Experimental and Modeling Results," *NASA Reference Publication 1274*, February, 1992.

2 Vogel, W. J., J. Goldhirsh, and Y. Hase, "Land-Mobile-Satellite Fade Measurements in Australia," Vol. 29, No. 1, pp. 123-128, Jan.-Feb., 1992.

3 Vogel, W. J., and J. Goldhirsh, "Mobile Satellite Propagation Measurements at L-Band Using MARECS-B2," *IEEE Trans. Antennas and Propagation*, Vol. 38, No. 2, pp. 259-264, February, 1990.

4 Goldhirsh, J., and W. J. Vogel, "Roadside Tree Attenuation Measurements at UHF for Land-Mobile Satellite Systems," *IEEE Trans. Antennas and Propagation*, Vol. AP-35, pp. 589-596, May, 1987.

5 Goldhirsh, J., and W. J. Vogel, "Mobile Satellite Fade Statistics for Shadowing and Multipath from Roadside Trees at UHF and L-Band," *IEEE Trans. Antennas and Propagation*, Vol. AP-37, No. 4, pp. 489-498, April, 1989.

6 Goldhirsh, J. and W. J. Vogel, "Mobile Satellite Propagation Measurements from UHF to K Band, *Proceedings of the 15th AIAA International Communications Satellite Systems Conference*, 28 February–3 March, 1994, San Diego, California, pp. 913–920.

7 Vogel, W. J., and J. Goldhirsh, "Earth-Satellite Tree Attenuation at 20 GHz; Foliage Effects," *IEE Electronics Letters*, Vol. 29, No. 18, 2 Sept. 1993.

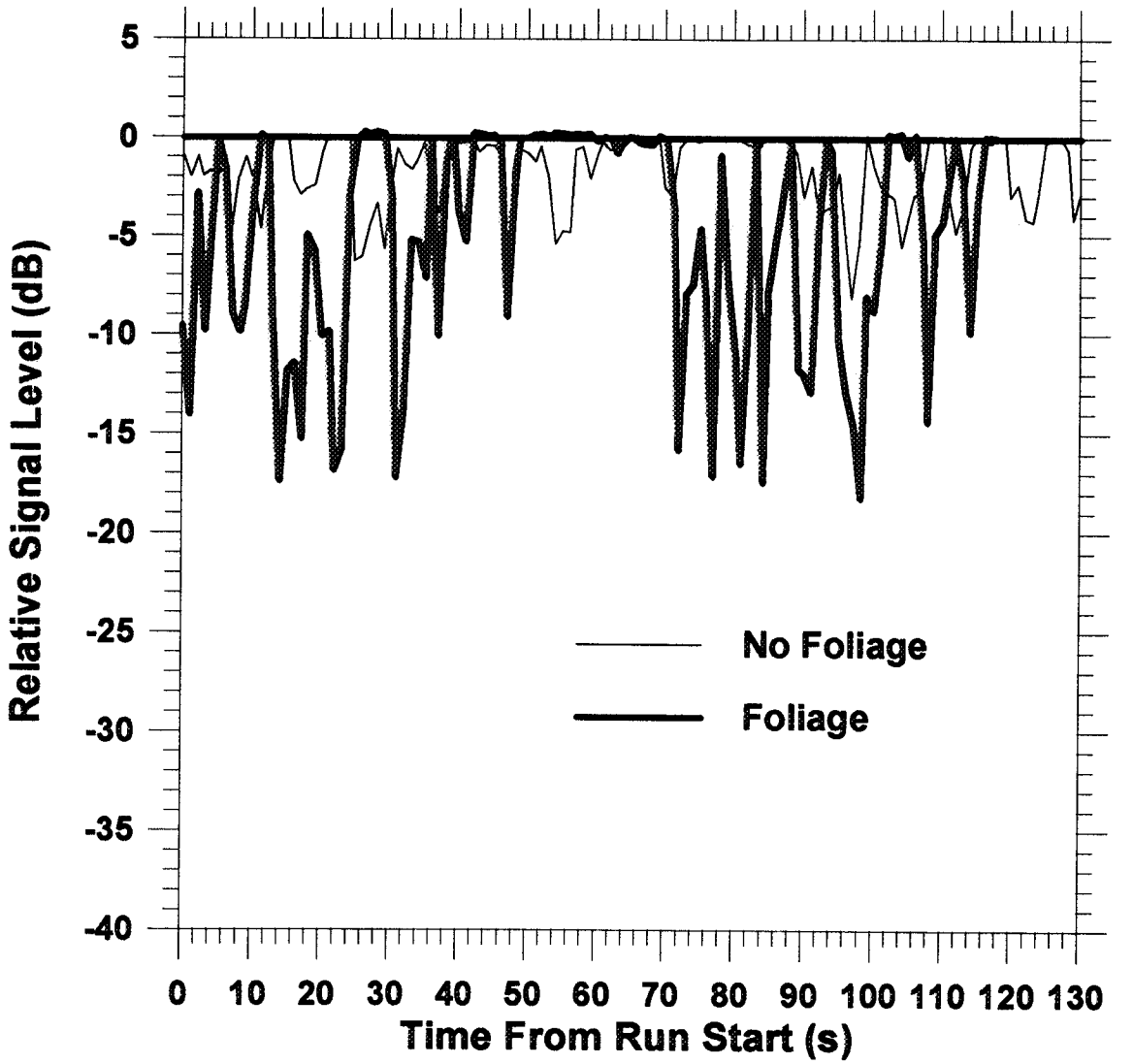

Figure 7: Comparison of average signal time-series runs for the full foliage (thick curve) and no foliage (thin curve) cases for 42nd Street run in Austin, Texas.

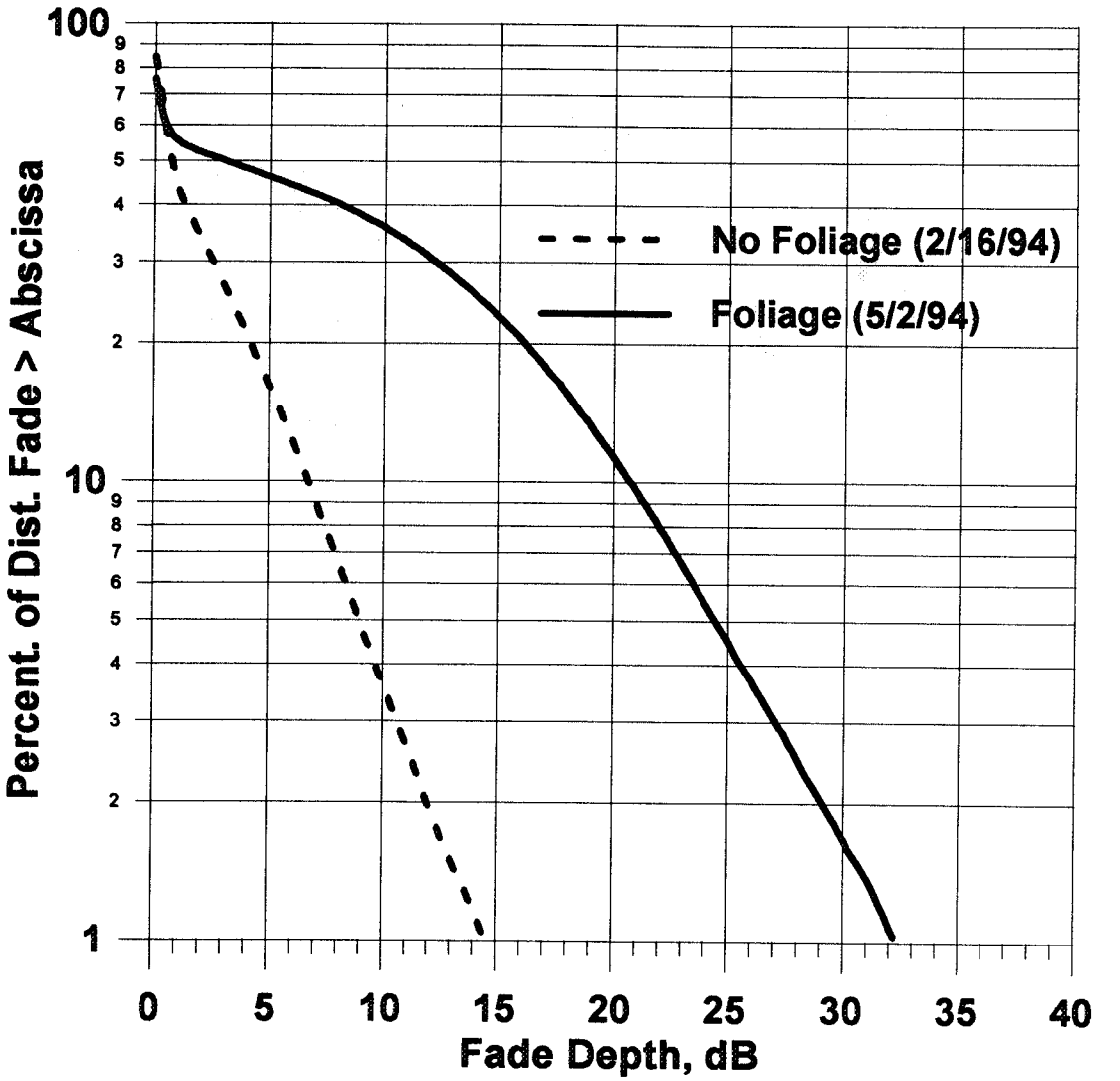

Figure 8: Cumulative distributions for foliage (thick curve) and non-foliage (thin curve) cases for 42nd Street run in Austin, Texas.